

Synthesis and characterization of lanthanum monoaluminate by co-precipitation method

L. Djoudi^{1,a}, M. Omari², N. Madoui²

¹Laboratory of Molecular chemistry and environment, University of Med Khider Biskra, Algeria

²Laboratory of Molecular chemistry and environment, University of Med Khider Biskra, Algeria

Abstract. Our contribution has focused on the synthesis and characterization of lanthanum monoaluminate LaAlO_3 by the method of co-precipitation. The powder was successfully synthesized using NaOH , $\text{La}(\text{NO}_3)_3 \cdot 6\text{H}_2\text{O}$ and $\text{Al}(\text{NO}_3)_3 \cdot 9\text{H}_2\text{O}$ as raw materials by this method and calcined at different temperatures. It was characterized by several techniques: Fourier transform infrared spectroscopy (FT-IR), thermogravimetric and differential thermal analysis (TGA/DTA), X-ray diffraction (XRD) and laser diffusion. All the results for physico-chemicals characterizations show that the crystallization temperature of the LaAlO_3 precursor gels precipitated is estimated as 790°C by TG/DTA. The XRD pattern of the LaAlO_3 precursor gels calcined at 700°C for 6 h has a perovskite structure of rhombohedral hexagonal phase formed and the presence of crystalline impurities is not found. The crystallite size of LaAlO_3 slightly increases from 31 to 44.5 nm with calcination temperature increasing from 700 to 1000°C for 6 h.

Key words. Lanthanum monoaluminate; method of coprecipitation; thermal analysis; perovskite; rhombohedral hexagonal; LaAlO_3 .

1 Introduction

Lanthanum aluminate (LaAlO_3) has attracted a great attention in recent years because of its variety of applications [1–8]. LaAlO_3 with a perovskite-type structure [9] is widely used as substrates and electrically insulating buffers for depositing high-temperature superconducting films due to its high quality factor and excellent lattice and thermal expansion matching ability [2, 6]. Its use as a gate dielectric material has also been explored [10, 11]. In addition, LaAlO_3 powder has been studied as a catalyst for oxidative coupling of methane and hydrogenation and hydrogenolysis of hydrocarbons due to its high catalytic activity [12]. Polycrystalline LaAlO_3 has been commonly prepared by a solid-state reaction method: i.e. direct mixing and firing of pure oxides of La_2O_3 and Al_2O_3 at temperature greater than 1550°C [13–16]. The full development of the LaAlO_3 phase has been exercised by only heating the sample to 1600°C and then reheating to 1750°C for 3 h to form a polycrystalline disk. The preparation of a buffer disk of 123 nm thick LaAlO_3 by radiofrequency magnetron sputtering has also been reported by Sung et al. [14].

^a e-mail : djoudi_lynda@yahoo.fr

Although the solid-state reaction is very simple, this process is not entirely satisfactory because of several serious drawbacks such as introduction of impurities during milling, high reaction temperature, limit of complete oxide reaction and chemical homogeneity, large particle sizes and low sintering ability [17, 18]. Therefore, extensive investigations have been performed for preparing finer and more homogeneous powders at lower temperatures using various chemical processes. Vidyasagar et al. [18] have obtained pure LaAlO_3 powders by calcining the precursor at $947\text{ }^\circ\text{C}$ for 12 h in air via urea solution route. Pure LaAlO_3 powders have been synthesized at $860\text{ }^\circ\text{C}$ using polyacrylamide by Douy and Odier [19]. Lux et al. [20] have also attempted to prepare LaAlO_3 powders by an aerosol-furnace technique, using water-soluble lanthanum and aluminum salts, and furnace temperature between 1200 and $1500\text{ }^\circ\text{C}$, where the formation of LaAlO_3 has been reported to be again only partial, and the sample still contains La_2O_3 and Al_2O_3 . Moreover, Taspinar and Tas [16] have also reported the synthesized pure LaAlO_3 powders by calcining at $750\text{ }^\circ\text{C}$ for 16 h, using a self propagating combustion method from aqueous solutions containing $\text{CH}_4\text{N}_2\text{O}$ and respective nitrates of lanthanum and aluminum. Furthermore, they have also synthesized pure LaAlO_3 powders at $850\text{ }^\circ\text{C}$ by the homogeneous precipitation from an aqueous solution containing $\text{CH}_4\text{N}_2\text{O}$ in nitrate salts [16]. Kakihana and Okubo [21] have reported that in the polymerization route of citric acid and ethylene glycol, pure perovskite LaAlO_3 has been obtained when the precursor is heat-treated in a furnace at $700\text{ }^\circ\text{C}$ for 8 h or at $750\text{ }^\circ\text{C}$ for 2 h. Furthermore, al Behera et al. [22] have produced spherical LaAlO_3 nanoparticles by a novel ultrasonic assisted combined gel synthesis from LaCl_3 and AlCl_3 solution with ammonia destabilization. On the other hand, the synthesis and luminescence properties of $\text{LaAlO}_3: 1\% \text{Eu}^{3+}$ nanocrystals have been discussed by Hreniak et al. [23]. They have pointed out the increasing luminescence life time with decreasing nanocrystals size. Moreover, the formation mechanism of the LaAlO_3 powders from aluminum hydroxide and lanthanum oxide using an evaporation process have been studied by Danchevskaya et al. [24]. They have demonstrated that LaAlO_3 has formed through the intermediate crystalline substances of oxyhydroxide LaOOH and hydroxide $\text{La}(\text{OH})_3$.

However, all these processes are either complex or expensive, and limit their large scale production. However, an extensive search on the sintering behavior of low-temperature synthesized LaAlO_3 nanopowders has been limited [17, 25, 26].

Chemical coprecipitation route is a simple method for synthesizing nanopowders [25]. The base precipitant most used in this method is NH_4OH .

Recently, Li et al. [17]; Nair et al. [26]; and Kuo *et al.* [8-27] have used this method to synthesize pure LaAlO_3 using the mixed solution of NH_4OH and calcined at 700, 800 and $1000\text{ }^\circ\text{C}$, respectively. However, the synthesis of lanthanum monoaluminate has been rarely reported using a mixture of sodium hydroxide such as base precipitant

In the present study, nanocrystalline LaAlO_3 powders have been successfully synthesized using the mixed solution of NaOH in low temperature range of $500\text{--}1000\text{ }^\circ\text{C}$ and pH 9. The preparation technique, thermal behavior, crystal structure, crystallite size, volume distribution of particle size, behavior of the low-temperature synthesized LaAlO_3 nanopowders have been discussed in detail.

2 Experimental procedure

2.1 Sample preparation

The starting materials were reagent-grade lanthanum nitrate [$\text{La}(\text{NO}_3)_3 \cdot 6\text{H}_2\text{O}$, purity 98%, supplied by BIOCHEM Chemopharma Montreal Quebec], aluminum nitrate [$\text{Al}(\text{NO}_3)_3 \cdot 9\text{H}_2\text{O}$, purity 99%, supplied by BIOCHEM Chemopharma Montreal Quebec] and hydroxide Sodium 12N [NaOH , purity 98%, supplied by BIOCHEM Chemopharma United Kingdom]. The aqueous solution was prepared from reagent-grade $\text{La}(\text{NO}_3)_3 \cdot 6\text{H}_2\text{O}$ and $\text{Al}(\text{NO}_3)_3 \cdot 9\text{H}_2\text{O}$ by dropping then slowly into the dilute hydroxide Sodium solution was used as the precipitant (pH 12) with vigorous agitation for 2.5h; the pH value was kept at 9 by adjusting the amount of NaOH to form white precipitates. In all cases, after the reaction was completed, the white precipitates were centrifugally washed thoroughly

for 10 min, four times with a distilled water and two times with ethanol, for each washing they were filtered then the resultant gelatinous precipitates were dried overnight at 110°C in oven .

The calcinations of the precursor powder LaAlO_3 was conducted in an Al_2O_3 boat in a temperature range of 500–1000° C for 6 h. at heating rate of 5 °C/min.

The flow chart for preparing LaAlO_3 nanoparticles by co-precipitation method is shown in Figure 1

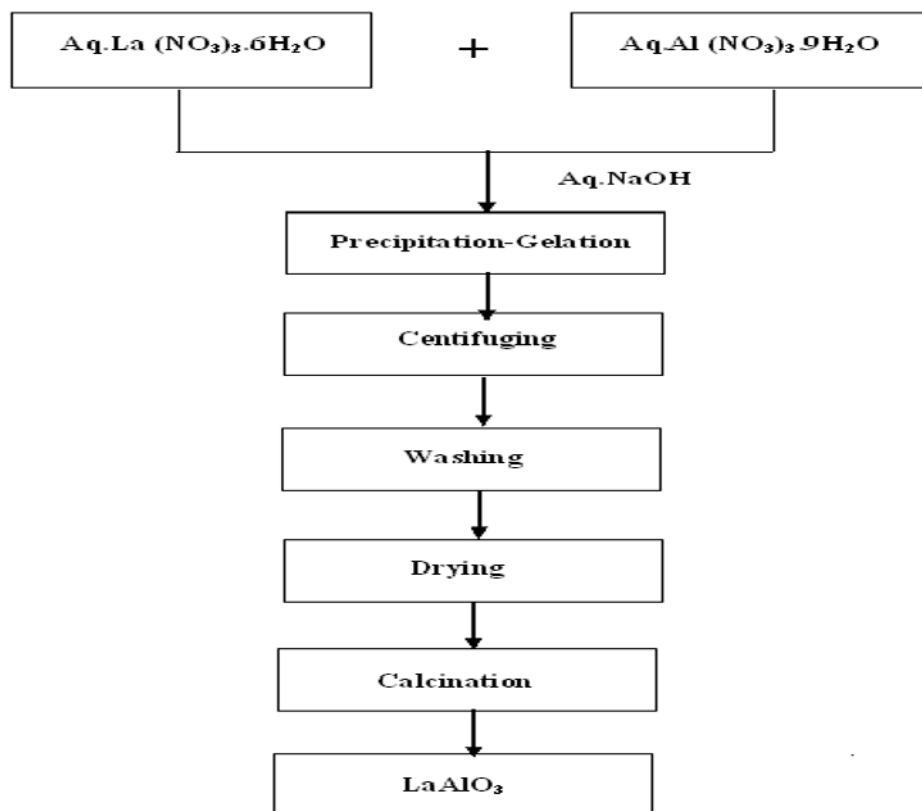


Fig. 1. Flow chart for preparing LaAlO_3 nanoparticles by co-precipitation method

2.2 Sample characterization

The thermal decomposition processes of the precursor gels were studied in air atmosphere by thermogravimetric and differential thermal analyses using TG/DTA, STAPT-1600 LINSEIS were conducted on a 50mg powder sample at a heating rate of 5 °C/min in air with Al_2O_3 powders as a reference material. The calcination temperature was determined from DTA. The Fourier transform infrared (FT-IR) absorption spectra were obtained by Processing on an optical bench of the standard PYE UMCAM PHILIPS FTIR spectrometer (4000–400 cm^{-1}). The samples were mixed in a KBr matrix (1:200) and pressed pellets and the spectra were averaged out from 64 scans with a nominal resolution of 2 cm^{-1} . X-ray diffraction (XRD) patterns were recorded using XRD, Model BRUKER – AXE type D8) with $\text{Cu K}\alpha$ radiation ($\lambda_{\text{K}\alpha}=1.54056 \text{ \AA}$) and a Ni filter, operated at an accelerating voltage of 40 kV, a current of 40mA and a scanning rate of .25°/min. The powder samples were mounted on a flat XRD plate and scanned at room temperature in the range 10°-90° to identify the crystalline phases present in the calcined powders By comparison with Joint Committee on Powder Diffraction Standards(JCPDS)files. The crystallite sizes of the powders were calculated from full-

width at half-maximum (FWHM) values from the most intense peak of the diffractogram, the (110) reflection in this case, using the Scherer formula [28].

$$D_{\text{XRD}} = \frac{0.9\lambda}{\beta \cos\theta} \quad (1)$$

Where D_{XRD} is the crystallite size in nm, λ is the radiation wavelength, θ is the diffraction peak angle and β is the corrected line width at half-peak intensity. The correction for instrumental peak broadening was made using the Warren formula: $\beta = (\mathbf{b}_{\text{obs}}^2 - \mathbf{b}^2)^{1/2}$, where \mathbf{b}_{obs} is the line width at half-peak intensity related to LaAlO_3 powder and \mathbf{b} is the line width of the (1 1 0) diffraction peak. Particles size distribution in solution was measured with a Malvern Mastersizer Hydro2000G granulometer. The equipment can measure grain sizes ranging from 0.02 to 2000 μm . The measurements are performed in an aqueous (water with added sodium hexametaphosphate (dispersant) with agitation and ultrasonic are applied for 15 min

3 Result and discussion

3.1 Thermal behavior and phase formation of the LaAlO_3 gel powders

Figure 2 illustrates the TG/DTA curves of the precursor powders heated at a rate of 5 $^\circ\text{C}/\text{min}$ in the temperature range between 50 and 1000 $^\circ\text{C}$ in static air. The TG curve shows the first weight loss at 330 $^\circ\text{C}$ (-18.80%) can be ascribed to the decomposition and burnout of most sodium nitrate in the precursor powders. The second weight loss (-8.8 %) between 400 and 520 $^\circ\text{C}$ is mostly due to the dehydration of the lanthanum and aluminum hydroxides. The weight loss between 520 and 750 $^\circ\text{C}$ with a clear plateau is presumably by the formation of an intermediate decomposition product and a small weight loss between 750 and 790 $^\circ\text{C}$ by the decomposition of residual nitrates involved in the intermediate product.

The DTA result in Figure 2 also reveals two main endothermic events at 130 and 490 $^\circ\text{C}$, respectively. At the temperature below 130 $^\circ\text{C}$ is assigned to the loss of moisture from the washed precursor powders [22]. The second endothermic peak at 490 $^\circ\text{C}$ is attributed to the decomposition of the lanthanum and aluminum hydroxides. The sharp exothermic peak at 790 $^\circ\text{C}$ is due to the formation of the LaAlO_3 .

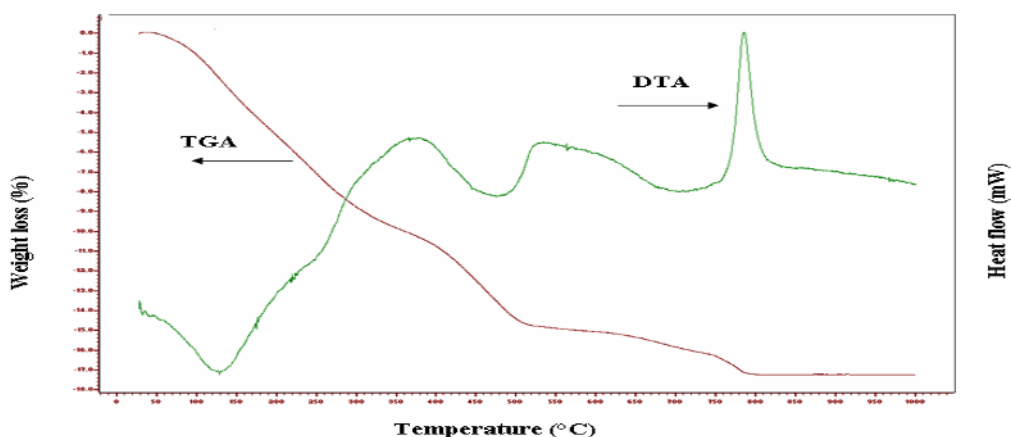


Fig. 2. DTA/TG curves of the LaAlO_3 precursor powders with a heating rate of 5 $^\circ\text{C}/\text{min}$.

Kakahana and Okubo [21] have synthesized the LaAlO_3 powders through the in situ polymerization route utilizing citric acid and ethylene glycol and found no clear exothermic peak corresponding to LaAlO_3 crystallization. On the other hand, Taspinar and Tas [16] have indicated that the crystallization temperature of LaAlO_3 measured by DTA is 992°C for the precursor powders prepared by the homogeneous precipitation process; so as *Kuo and al* [8,27] have indicated that the crystallization temperature of LaAlO_3 measured by DTA is 810°C for the precursor powders prepared by co-precipitation process. The distinction between the present and other reports [8, 16, 21,27] can be caused by different process routes creating various crystallization temperatures in the DTA curves [8] ; Moreover at various heating rates is found that the exothermic peak shifts to high temperature with increasing heating rate which is demonstrated by *Kuo and al*. This phenomenon suggests that irregular lanthanum and aluminum ions are rearranged into the periodic lattice of the growing crystal. When the heating rate increases the rearrangement is delayed to the high temperature side [27].

3.2 Infrared spectra

IR analysis of synthesized samples is important both for the control of the reaction process and of the properties of materials obtained. The FT-IR absorption spectra of the LaAlO_3 precursor powders, calcined at various temperatures for 6h are shown in Figure 3. The spectrums between 3600 and 3200 cm^{-1} in Figure 3 (a), (b), (c) and (d) are related to the stretching vibration of the free hydroxyl group. Also indicates the presence of adsorbed water [29]. The characteristic nitrate stretching frequencies at $1700\text{--}1600\text{ cm}^{-1}$. However, the peaks due to the stretch vibrations in NO_3^- at $1410\text{--}1360\text{ cm}^{-1}$ (strong bands) [30, 31] are shown in Figure 3 (a),(b) ,(c) and (d) are evident. In the $700\text{--}400\text{ cm}^{-1}$ region of the IR spectrum is shown in Figure 3 (a), (b) ,(c),(d) and (e) ,the observed specific peaks at $681,676,667,596, 458,$ and 447 cm^{-1} may be attributed to the characteristic M–O (Possibly La–O and Al–O stretching frequencies) vibrations for the perovskite structure compounds [32].

After the LaAlO_3 powders calcined at 700°C is shown in Figure 3 (e), the only distinguishable transmittance bands detected in the specimen were those for LaAlO_3 (the characteristic bands at 667 and 447 cm^{-1}) [33, 34]. XRD analysis (refer to Figure 4) confirmed the formation of crystalline LaAlO_3 at 700°C .

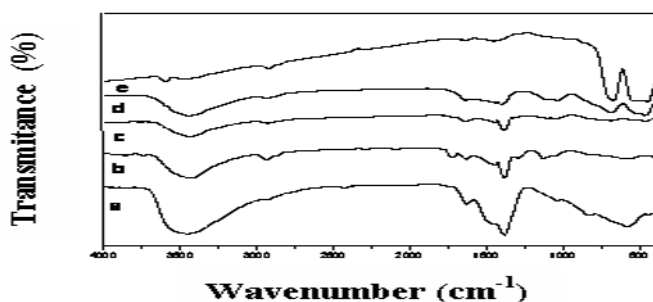


Fig. 3. FT-IR absorption spectra of the LaAlO_3 precursor powders, calcined at various temperatures for 6h: (a) room temperature, (b) 200°C , (c) 500°C , (d) 600°C and (e) 700°C .

3.3 Phase characterization of the LaAlO_3 precursor powders after calcined

Figure 4 illustrates the XRD patterns of the LaAlO_3 powders calcined at different temperatures for 6h. The XRD pattern of the LaAlO_3 powders calcined at 500°C for 6h is shown in Figure 4 (a), which reveals that the calcined powders are still amorphous.

The absence of peaks corresponding to $\text{La}(\text{OH})_3$ or $\text{Al}(\text{OH})_3$ indicates the amorphous nature of the precipitated hydroxides. Figure 4(b) indicates that after calcined at 600 °C for 6 h, the crystalline phase is the rhombohedral LaAlO_3 with poor crystallinity. When the LaAlO_3 precursor powders calcined at 700–1000 °C (Figure 4 (C), (d), (e) and (f)), shows good crystallinity. These XRD peaks correspond to reflections from pure rhombohedral LaAlO_3 with a perovskite structure. They are in good agreement with JCPDS card 31-0022. Moreover, the result of Figure 4 also reconfirms that the exothermic peak of Figure 2, spanning from 740 to 820 °C, is due to the formation of the rhombohedral of LaAlO_3 nanopowders.

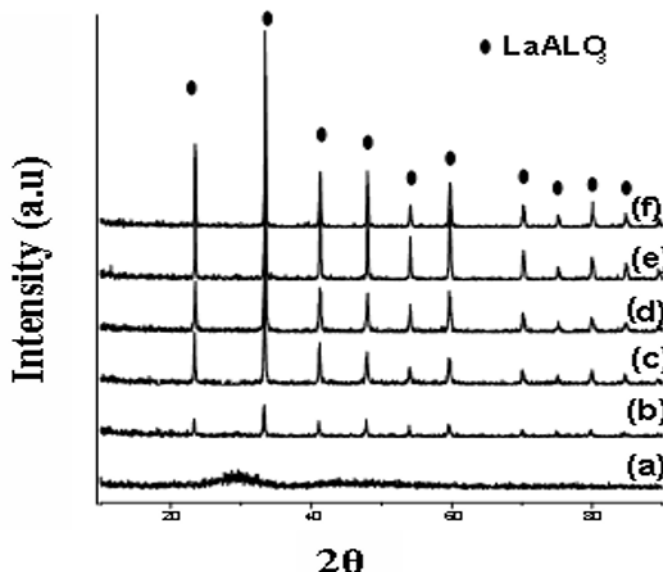


Fig. 4. XRD patterns of the LaAlO_3 precursor powders calcined at different temperatures for 6 h: (a) 500 °C, (b) 600 °C, (c) 700 °C, (d) 800 °C, (e) 900 °C and (f) 1000 °C .

Furthermore, Figure 4 indicate that the XRD patterns of the calcined LaAlO_3 precursor powders are representative of LaAlO_3 , and no reflections from La_2O_3 and Al_2O_3 are observed as distinct intermediate phases period to the formation of LaAlO_3 during the thermal decomposition of the precursor powders even at 1000° C [22]. Kakihana and Okubo [21] have pointed out that no detection of La_2O_3 and Al_2O_3 implies almost perfect mixing of the constituent cations in the precursor powders. They have also indicated that LaAlO_3 does not form through a solid-state reaction between isolated La_2O_3 and Al_2O_3 fine particles but forms directly from the amorphous precursor powder without significant segregation of individual materials [21]. Moreover, in the present study, the intermediate crystalline substances of LaOOH and $\text{La}(\text{OH})_3$ are not observed; this is consistent with the results of *Kuo and al* [8, 27]. On the other hand this result contradicts to that of *Danchevskaya et al.* [24].

The relation between phase and calcination temperature of the low-temperature synthesized LaAlO_3 powders has been examined earlier by XRD [16–18, 20, 21]. Taspinar and Tas [16] have successfully synthesized LaAlO_3 powders by two chemical preparation techniques: (i) homogeneous precipitation from aqueous solutions containing urea ($\text{CH}_4\text{N}_2\text{O}$) in the presence of nitrate salts and (ii) self-propagation combustion synthesis (SPCS) from aqueous solutions containing $\text{CH}_4\text{N}_2\text{O}$ and respective nitrate salts of lanthanum and aluminum. In the homogeneous precipitation process, when calcined up to 700 °C, the La_2O_3 phase is still detected and completely converted to pure LaAlO_3 at 850 °C. Therefore, 750 °C is the lowest temperature necessitated for the formation of LaAlO_3 powders by the SPCS route. Li et al. [17] have used $\text{La}(\text{NO}_3)_3$ and $\text{Al}(\text{NO}_3)_3$ as raw materials and kept pH about at 9 in the coprecipitation method. Pure LaAlO_3 powders have been obtained after

calcined at 700 °C for 32 h or 800 °C for 2 h using hydroxide, cyanide and nitrate solid solution precursors as the starting materials. The appearance of LaAlO₃ is observed when calcined at 947 °C for 12 h in air, as reported by Vidyasagar et al. [18]. Furthermore, Lux et al. [20] have used reagent-grade lanthanum nitrate and aluminum nitrate as the starting materials. The XRD data on the aerosol-derived particles indicate that the material is amorphous until processing temperatures exceed about 900 °C. In this case, the crystalline phases observed by XRD are the major lanthanum oxide and minor LaAlO₃ phases when calcined at 1200 °C. If calcined up to 1500 °C, the major phase is LaAlO₃, but lanthanum and aluminum oxide phases are still in evidence [20]. Moreover, Kakihana and Okubo [21] have obtained the LaAlO₃ precursor by heating a mixed solution of citric acid, ethylene glycol and nitrates of lanthanum and aluminum. The formation of pure perovskite LaAlO₃ has occurred when the precursor is calcined at 700 °C for 8 h or at 750 °C for 2 h. There is no XRD evidence for the presence of crystalline impurities.

The present investigation has used the mixed solution of NaOH, lanthanum nitrate and aluminum nitrate, precipitation at pH 9, calcination at 700 °C for 6 h and then obtained pure perovskite LaAlO₃ this result is in good agreement with *Kuo et al*, but being the lowest temperature chemical coprecipitation so far the lowest among others.

3.4 Crystallite size and distribution by volume particle size of LaAlO₃ powder

Table 1 shows the variation of average crystallite size (D_{XRD}) of the LaAlO₃ powders calcined at different temperatures for 6 h. The crystallite sizes calculated from the Scherrer formula are slightly increase in the range of 31–44.50 nm respectively with the calcination temperature increasing from 700 to 1000°C. On the other hand this result is lower than calculated by *Kuo and al*. This distinction can be caused of synthesis parameters such as chemical nature of the base precipitant that affects on the morphological characteristics of the nanoparticles LaAlO₃ powders.

Table 1. Variation of crystallite size of the LaAlO₃ powders calcined at different temperatures for 6h

Calcination temperature(°C)	Crystallite size (nm)
700	31
800	34.28
900	41.04
1000	44.50

Figure 5 shows that the particle size distribution in volume of LaAlO₃ powder calcined at different temperature 800 to 1000°C, the average diameters in volume $D_v(0.5) = 0.22; 0.25; 0.25 \mu\text{m}$ respectively. This result also indicates that the powders are highly agglomerated. This is could be due to the agglomeration of ultra-fine powders, present in the suspension. Since the LaAlO₃ gel powders are prepared through the wetchemical route; the agglomeration takes place during processing.

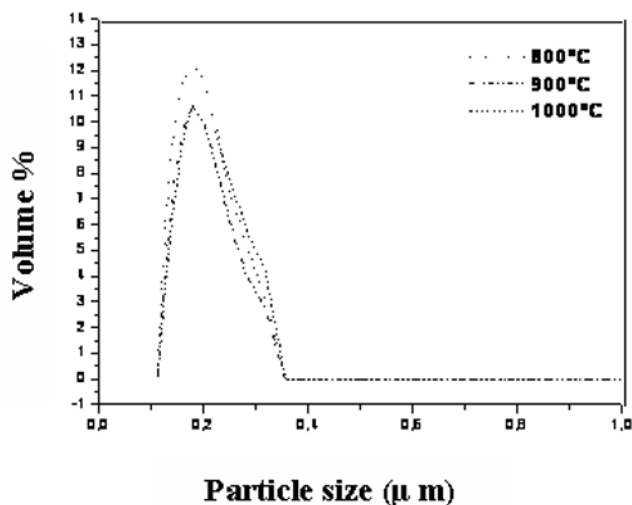


Fig. 5. Particle size distribution in volume of LaAlO₃ powder calcined at different temperature 800 to 1000°C

4 Conclusions

Nanocrystalline lanthanum monoaluminate powders have been successfully synthesized at low temperature by chemical coprecipitation using a mixture of sodium hydroxide, lanthanum and aluminum nitrate solutions. When the LaAlO₃ precursor powders are precipitated at pH 9 and calcined at 700°C for 6 h, the pure perovskite LaAlO₃ is obtained. No reflection peaks of La₂O₃ and Al₂O₃ are observed. The calcination temperature of 700 °C is so far the lowest process temperature for complete LaAlO₃ formation. The nanocrystallite size slightly increase from 31 to 44.5 nm with the calcination temperature increasing from 700 to 1000 °C, for the LaAlO₃ precursor powders calcined for 6 h.

References

1. T. Tagawa, H. Imai, Mechanistic aspects of oxidative coupling of methane over LaAlO₃, J. Chem. Soc. **84**, 923–929 (1988).
2. G. Y. Sung, K. Y. Kang, S. C. Park, J. Am. Ceram. Soc. **74**, 437–439 (1991).
3. S.-Y. Cho, I. T. Kim, K. S. Hong, J. Mater. Res. **14**, 114–119 (1999)
4. D. A. Atwood, B. C. Year wood, J. Organomet. Chem. **600**, 186–197 (2000).
5. C.-S. Hsu, C. L. Huang, Effect of CuO additive on sintering and microwave dielectric behavior of LaAlO₃ ceramics, Mater. Res. Bull. **36**, 1939–1947 (2001).
6. M. Nieminen, T. Sajavaara, E. Rauhala, M. Putkonen, L. Niinisto, J. Mater. Chem **11**, 2340–2345 (2001).
7. Q. X. Fu, F. Tietz, P. Lersch, Solid State Ionics **117**, 1059–1069 (2006).
8. C. L. Kuo, C. L. Wang, T. Y. Chen, G. J. Chen, I. M. Hung, C. J. Shih, K. -Z. Fung, J. Alloys Compds. **440**, 367–374 (2007).
9. S. Geller, V. B. Bala, Acta Cryst. **9**, 1019–1025 (1956).
10. X. Lu, Z. Liu, Y. Wang, Y. Yang, X. Wang, H. Zhou and B. Nguyen, J. Appl. Phys. **94** (2), 1229–1234 (2003).
11. B. Park and H. Ishiwara, Appl. Phys. Lett., **82**(8), 1197–1199 (2003).

12. T. Tagawa and H. Imai, J. Chem. Soc., Faraday Trans. 1. Phys. Chem. Condens. Phases, **84**(4), 923–929 (1988).
13. S. Geller, B. V. Bala, Acta Crystallogr. **9**, 1019(1956).
14. G. Y. Sung, K. Y. Kang, S. C. Park, J. Am. Ceram. Soc. **74** (1991) 437.
15. M. Mizuno, T. Yamada, T. Noguchi, Yogyo Kyokaish. **82**, 630 (1974).
16. E. Taspinar, A. C. Tas, J. Am. Ceram. Soc. **80**, 133-141 (1997).
17. W. Li, M. W. Zhuo, J. L. Shi, Mater. Lett. **58**, 365–368 (2004).
18. K. Vidyasagar, J. Gopalakrishnan, C. N. R. Rao, J. Solid State Chem. **58**, 29 (1989).
19. A. Douy, P. Odier, Mater. Res. Bull. **24**, 1119 (1989).
20. B. C. Lux, R. D. Clark, A. Salazar, L. K. Sveum, M. A. Krebs, J. Am. Ceram. Soc. **76** (1993) 2669.
21. M. Kakihana, T. Okubo, J. Alloys Compd. **266** (1998) 129.
22. S. K. Behera, P. K. Sahu, S. K. Pratihari, S. Bhattacharyya, Mater. Lett. **58** (2004) 3710.
23. D. Hreniak, W. Strek, P. Deren, A. Bednarkiewicz, A. Kukowiak, J. Alloys Compd. **828**, 408–412 (2006).
24. M. N. Danchevskaya, Yu. D. Ivakin, S. N. Torbin, G. P. Muravieva, O. G. Ovchinnikova, J. Mater. Sci. **41**, 1385(2006).
25. M. A. C. G. van de Graaf, J. H. H. ter Matt, A. J. Burggraaf, J. Mater. Sci. **20**, 1407 (1985).
26. J. Nair, P. Nair, F. Mizukami, J. G. V. Ommen, G. B. M. Doesburg, J. R. H. Ross, A. J. Burggraaf, J. Am. Ceram. Soc. **83**, 1942 (2000)
27. Chia-Liang Kuo, Yen-Hwei Chang, Moo-Chin Wang Crystallization kinetics of lanthanum monoaluminate (LaAlO₃) nanopowders prepared by co-precipitation process Ceramics International **35**, 327–332 (2009)
28. H. P. Klug, L. E. Alexander, *X-ray Diffraction Procedures*, John Wiley and Sons, New York, (1974).
29. A. Baranauskas, D. Jasaitis, A. Kareiva, Characterization of sol–gel process in the Y–Ba–Cu–O acetate–tartrate system using IR spectroscopy, *Vibr. Spectrosc.* **28** (2), 263 (2002).
30. J. Livage, M. Henry, C. Sanchez, Sol–gel chemistry of transition metal oxides, *Prog. Solid State Chem.* **18** (4), 259 (1988).
31. C. J. Brinker, G. W. Scherrer, *Sol–Gel Science: The Physics and Chemistry of Sol–Gel Processing*, Academic Press, Inc; New York, 59-64 (1990).
32. B. Schrader (Ed.), *Infrared Raman Spectroscopy: Methods and Applications*, VCH, Weinheim, (1995).
33. A. K. Adak, P. Pramanik, Mater. Lett. **30**, 269–273 (1997).
34. D. Zhou, G. Huang, X. Chen, J. Xu, S. Gong, Mater. Chem. Phys. **84**, 33–36 (2004).